

We are IntechOpen, the world's leading publisher of Open Access books Built by scientists, for scientists

4,800

Open access books available

122,000

International authors and editors

135M

Downloads

Our authors are among the

154

Countries delivered to

TOP 1%

most cited scientists

12.2%

Contributors from top 500 universities



WEB OF SCIENCE™

Selection of our books indexed in the Book Citation Index
in Web of Science™ Core Collection (BKCI)

Interested in publishing with us?
Contact book.department@intechopen.com

Numbers displayed above are based on latest data collected.

For more information visit www.intechopen.com



Exciton Dynamics in High Density Quantum Dot Ensembles

Osamu Kojima
Kobe University
Japan

1. Introduction

Remarkable progress has been made in the fabrication of semiconductor quantum dots (QDs) using the self-assembling method in lattice-mismatched material systems; they are based on the Stranski-Krastanow growth mode (Goldstein et al., 1985). In this process, initial two-dimensional growth transforms into three-dimensional growth. Using the self-assembling technique, it is possible to fabricate semiconductor nanostructures in a continuous growth process in a vacuum. The self-assembled QDs grown on a semiconductor substrate can offer the possibility of realizing various interesting devices such as QD lasers, ultrafast optical switches, and solar cells (Arakawa & Sakaki, 1982; Huffaker et al., 1998; Prasanth et al., 2004; Bogaart et al., 2005; Martí et al., 2006; Oshima et al., 2008). To realize such QD devices, it is necessary to design the optical properties by controlling the exciton characteristics and to fabricate high-quality and high-density QDs. From this viewpoint, we have clarified that the photoluminescence (PL) characteristics of excitons in multiple stacked QDs fabricated by using the strain compensation technique (Akahane et al., 2002, 2008, 2011) can be controlled by changing the QD separations along the growth direction (Nakatani et al., 2008; Kojima et al., 2008). In this chapter, we introduce the control method of excitonic characteristics by using the overlap of electron envelope functions between QDs along the growth direction.

2. Sample structures

We used three samples in this study. For each sample, InAs self-assembled QDs with 30 periods was grown on an InP(311)B substrate, as shown in Fig. 1, by solid-source molecular beam epitaxy using a strain compensation technique (Nakatani et al., 2008; Kojima et al., 2008, 2010, 2011). After growing a 150-nm thick $\text{In}_{0.52}\text{Al}_{0.48}\text{As}$ buffer layer, 4-ML InAs QDs were deposited. The samples have $\text{In}_{0.5}\text{Ga}_{0.1}\text{Al}_{0.4}\text{As}$ spacer layers with thicknesses (d) of 20, 30, and 40 nm. Hereafter, we will call these samples $d=X$ nm sample ($X=20, 30,$ and 40). The spacer layer compensates the stress caused by the lattice mismatch to a QD layer. The QD density in each layer is $3.4 \times 10^{10}/\text{cm}^2$.

3. Control of optical characteristics of excitons in QD ensembles

Figure 2 shows the spacer-layer-thickness dependence of the PL spectra at 3.4 K (Kojima et al., 2008). The PL measurement was performed by using a mode-locked Ti:sapphire pulse

laser. The emitted light was dispersed by a 32 cm single monochromator with a resolution of 1.0 nm. The PL intensity and peak energy clearly depend on the spacer layer thickness. With a decrease in the spacer layer thickness, the PL intensity decreases. The integrated intensity of PL band is plotted as a function of d in the inset of Fig. 2 for the clarification of the relation between the intensity of the PL band and d . The dotted line indicates the linear dependence of the intensity on d . The PL intensity is almost linearly proportional to d . It is well known that a decrease in the relative motion of electron and holes in systems of quantum wells or QDs causes an increase in the oscillator strength in the strong confinement regime because the oscillator strength is proportional to the probability of finding an electron and hole at the same position. Namely, since the overlapping of the envelope functions of the confined electron and hole is enlarged in each QD, the oscillator strength of QD excitons is approximately inversely proportional to the confinement volume (Takagahara, 1987; Kayanuma, 1988).

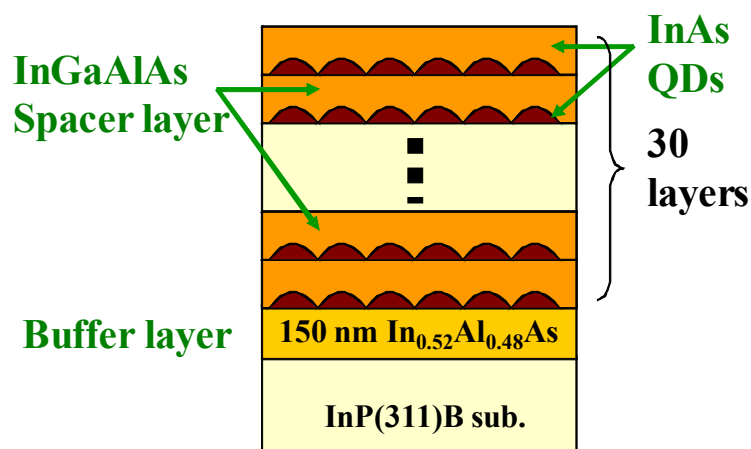


Fig. 1. Schematic of the sample structure.

Here, we discuss the origin of the confinement volume change. There are two possible factors for causing the expansion: (i) the creation of larger QDs owing to a decrease in d and (ii) the growth-direction elongation of the envelope function of confined carriers. It has been reported that larger-sized QDs are created in the case of the thinner capping layer (Xie et al., 1995; Saito et al., 1998; Persson et al., 2005). Indium atoms have a strong tendency to segregate at the surface when GaAs is deposited over InAs at temperature ~ 500 °C (Brandt et al., 1992), so that the capped InAs QD size tends to be small by a thick cap layer (Xie et al., 1995; Inoue et al., 2008). In addition, the thinner cap layer results in less compressive stress in the QDs (Saito et al., 1998; Persson et al., 2005), leading the strain-relaxed larger QDs. If a change in d causes this QD size variation due to the indium segregation or strain reduction, the magnitude of overlap of the envelope functions of confined electron and holes varies according to the change in the QD size. Since the oscillator strength depends on the QD size as described above, the PL intensity is expected to correspond to the variation of d . However, such possibility of the change in the QD size is denied as follows. The indium segregation is suppressed when the InAs QDs are capped by the indium alloys (Kim et al., 2003) so that in our samples, InGaAlAs spacer layer suppresses the indium segregation. Moreover, we employed the strain compensation technique in the QD growth, which means that the compressive strain to QDs is independent of d is practically independent. Therefore, we can focus on the growth-direction elongation of the envelope functions of confined carriers.

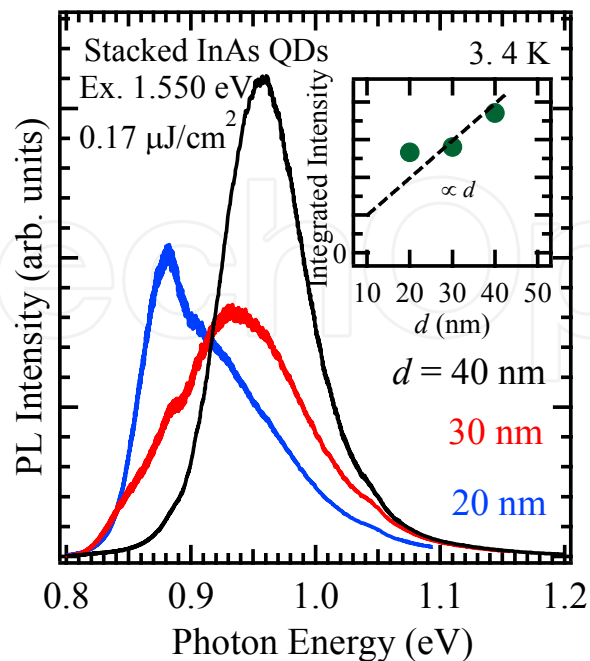


Fig. 2. The spacer-layer-thickness dependence of the PL spectrum in the stacked InAs QDs with $d=20, 30,$ and 40 nm at 3.4 K. The inset shows the d dependence of the integrated intensity of the PL bands. The dotted line denotes the linear dependence of the intensity on d .

The heavy holes forming excitons are strongly localized in each of QDs (Saito et al., 2005) because of the heavier mass. On the other hand, since the effective mass of an electron is less than that of a hole, the electron envelope functions are sensitive to the quantum confinement effect. When the spacer layer thickness decreases, the electrons approach each other along the growth direction, and the electron envelope functions overlap within the spacer layer. Consequently, it is considered that the electron envelope functions in the samples with 30 QD layers separated by thinner spacer layers interconnect weakly along the growth direction owing to the overlap. This interconnection results in the lowering of the oscillator strength because of the reduction in the magnitude of the overlap integral between the electron and hole envelope functions.

The interconnection of electron envelope functions induces the lower-energy shift and broadening of PL band, as shown in Fig. 2. In Fig. 2, since the electrons in the $d=40$ nm sample are practically isolated within each QD, we can conclude that the PL band at around 0.95 eV in the $d=40$ nm sample is typical for our QDs. The peak energy shift in the thinner d samples comes from the reduction in the confinement effects by the expansion of the confinement volume owing to the interconnection of electron envelope functions. In addition, the PL band broadens and the shape becomes asymmetric owing to the appearance of a new PL band at low energy side below 0.9 eV in Fig. 2. In the $d=20$ nm sample, the PL band clearly shows two components. As described above, the PL band around 0.95 eV results from the uncoupled QDs. Thus, the PL band below the energy of 0.9 eV arises from the interconnection of the electron envelope function.

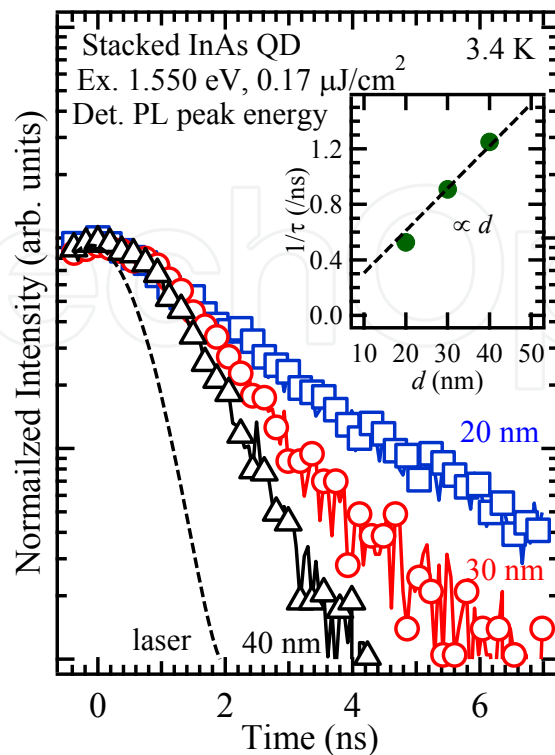


Fig. 3. The PL decay profiles observed at the peak energy in each sample. The dotted curve indicates the laser profile. The inset indicates the relation between $1/\tau$ and d . The dotted line denotes the linear dependence of $1/\tau$ on d .

When the above consideration is correct, the PL decay time should be inversely proportional to the spacer layer thickness. The spacer-layer-thickness dependence of the PL decay profile observed at a peak energy in each sample is shown in Fig. 3 (Kojima et al., 2008). The PL decay profiles were measured by a time-correlated single-photon counting method with a time resolution of 0.8 ns. The excitation source was a mode-locked Ti:sapphire pulse laser delivering 110 fs pulses with a repetition rate of 4 MHz. We used a pulse picker to reduce the laser repetition rate from 80 to 4 MHz. The excitation photon energy was 1.550 eV and the excitation density was $0.17 \mu\text{J}/\text{cm}^2$. PL was dispersed by a 27-cm single monochromator with a resolution of 1.0 nm and detected by a time-to-amplitude converter system with the use of a liquid-nitrogen-cooled InP/InGaAsP photomultiplier. All profiles are normalized by the PL intensity observed at 0 ns. The dotted curve shows a laser profile. The PL decay profile has a single component and it clearly depends on d . The evaluated PL decay times τ_d obtained by fitting with a single exponential function are 1.9, 1.1, and 0.8 ns in $d=20, 30,$ and 40 nm, respectively. This result is very different from that observed in the case of QD molecules. In the case of excitons in the QD molecules, the PL decay time decreases with a decrease in the interdot distance because of the superradiance effect (Bardot et al., 2005). In the inset of Fig. 3, $1/\tau_d$ was plotted as a function of d . The dotted line indicates the linear dependence of $1/\tau_d$ on d . τ_d of the QD excitons is inversely proportional to the oscillator strength f as described by the following equation (Andreani et al., 1999; Hours et al., 2005):

$$f = \frac{1}{\tau} \frac{3\pi\epsilon_0}{n} \frac{2mc^3}{e^2\omega_0^2} \quad (1)$$

where ω_0 is the optical transition frequency, n is the refractive index, and m is the free-electron mass. Hence, the relation between τ and d strongly supports our consideration that the elongation of the electron envelope function results in the lowering of the oscillator strength.

4. Temperature dependence of excitons in QD ensembles

The reduced oscillator strength of excitons in QD ensembles with interconnection effects may not be suitable for light-emission devices such as LEDs, laser devices, and so on without a further increase in the number of the stacking layer. However, some devices such as quantum information devices and solar cells require a long exciton lifetime. Thus, the controllable long exciton lifetime described in previous section is considered to be a noteworthy property of interconnected QDs for realizing novel devices. Here, we focus on a carrier dynamics depending on the temperature in order to clarify the effects of the interconnection in vertically aligned QD ensembles.

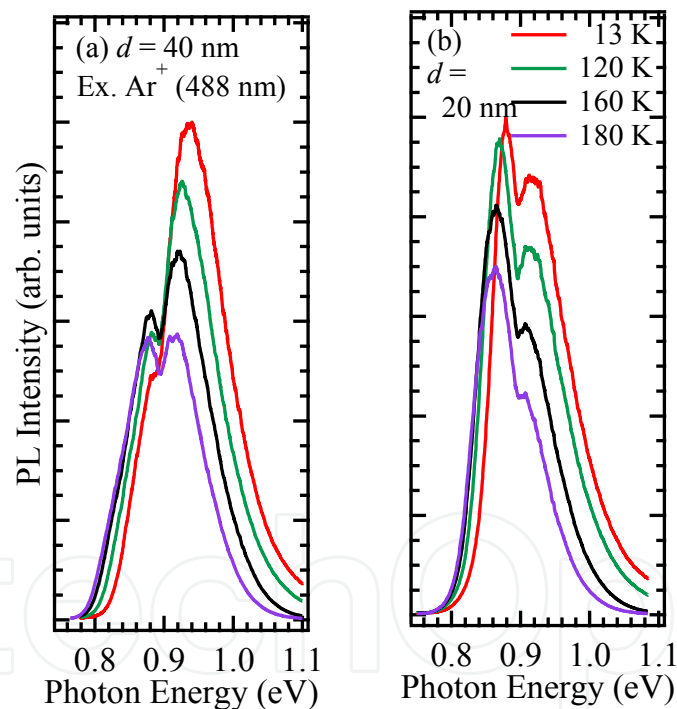


Fig. 4. Temperature dependence of the PL spectra in (a) the $d=40$ nm and (b) the $d=20$ nm samples. The dip at around 0.9 eV originates from the hydroxy group in the optical fiber.

Figure 4 (a) and 4 (b) show the temperature dependence of the PL spectra in the $d=40$ nm and 20 nm samples, respectively (Kojima et al., 2010). The PL measurement was performed by using the 488 nm line of a CW Ar^+ laser. The excitation density was kept at 10 W/cm^2 . The emitted light was dispersed by a 32-cm single monochromator with a resolution of 1.0 nm and was detected by using a liquid-nitrogen-cooled InGaAs-photodiode array. All spectra were normalized by the maximum intensity of the spectra at 13 K in each sample. The dip at around

0.9 eV is due to absorption by the hydroxy group in the optical fiber. The decrease in the PL intensity with an increase in the temperature in the $d=20$ nm sample is same as that in the $d=40$ nm sample. This result indicates that the nonradiative recombination process induced by an increase in the temperature is similar in both the samples.

In order to clarify the difference between the temperature dependences in both samples, we measured the PL decay profiles at various temperatures, as shown in Fig. 5. All the profiles were recorded at the PL peak energy. The PL decay times of both samples increase with the temperature. In Fig. 5 (c), the PL decay times of both samples are plotted as a function of temperature. The increase in PL decay time indicates that the growth by the strain compensation technique can suppress the generation of nonradiative centers with QD stacking. However, the temperature dependence of the PL decay time in the $d=20$ nm sample is different from that in the $d=40$ nm sample.

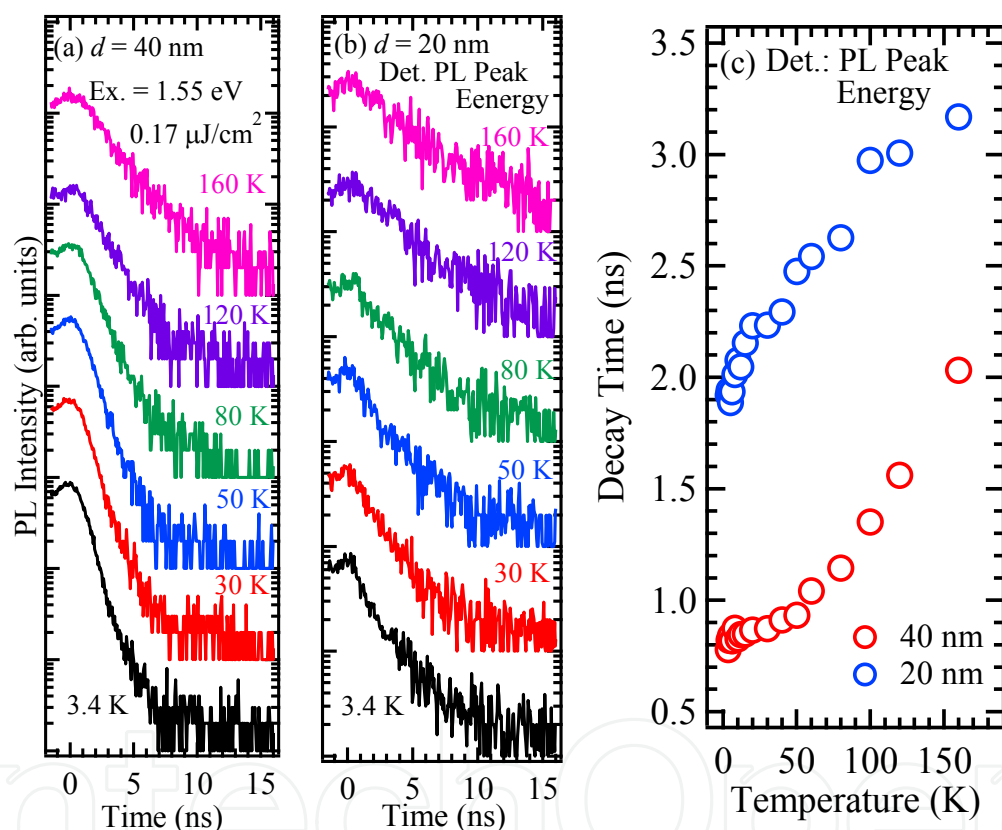


Fig. 5. Temperature dependence of the PL decay profiles in (a) $d=40$ nm and (b) $d=20$ nm samples. Each profile was recorded at the PL peak energy. (c) The PL decay times in both the samples are plotted as a function of temperature.

The increase in the PL decay time with the temperature is generally explained by the thermal dissociation of excitons into the electron-hole pairs, in which the excitons escape from the QDs into the spacer layer and/or the upper subband levels of electron and holes via thermionic emission (Wang et al., 1994; Yu et al., 1996; Fiore et al., 2000; Hostein et al., 2008), which is described as lateral coupling model. We considered that the temperature dependence of the PL decay time in the $d=40$ nm sample can be explained by this lateral coupling model. However, the temperature dependence of the PL decay time in the $d=20$ nm sample should include another factor, namely, the interconnection effect of the electron envelope functions.

In Fig. 6, the PL decay times in the low temperature region were plotted as a function of temperature. The PL decay time in the $d=40$ nm sample shows the almost constant value. This is the typical result for localized excitons. On the other hand, the PL decay time in the $d=20$ nm sample indicates the $T^{0.5}$ dependence as shown by the solid curve, which is similar property of the excitons in the quantum wires (Akiyama et al., 1994). This is an evidence of the QD interconnection. Therefore, the difference of the temperature dependence of the PL decay time in Fig. 5(c) arises from the dimensionality of excitons.

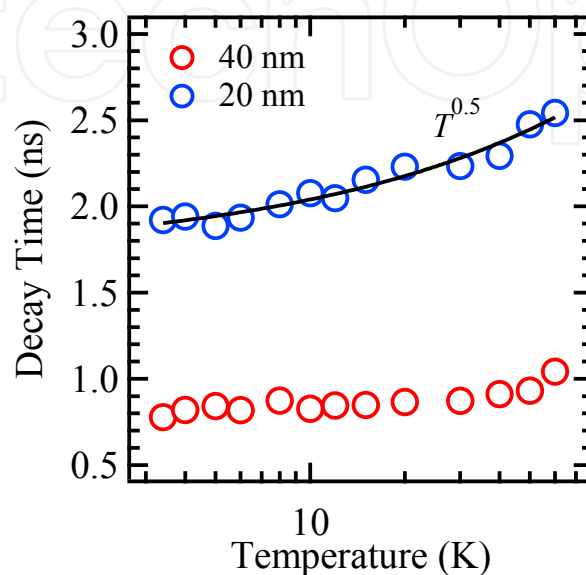


Fig. 6. Temperature dependence of the PL decay time around low temperature region.

Figure 7 shows the detection-energy dependence of the PL decay time in the $d=40$ nm sample measured at various temperatures (Kojima et al., 2011). For reference, the PL spectrum at 3.4 K is depicted. Even at 50 K, corresponding to 4.3 meV, the PL decay time depends on the detection energy; the lateral coupling occurs. Moreover, the increase factor of the decay time is enhanced at 100 K, which indicates the enhancement of the lateral coupling due to thermal activation of carriers.

If the lateral coupling originates only from the exciton/carrier transfer due to the thermal dissociation, the 50 K temperature is considered to be insufficiently to cause the lateral coupling. Therefore, it was deduced that the hole injection from the spacer layers to QDs results in the lateral coupling-like behaviour in the detection-energy dependence at lower temperature region. Assuming the strain distribution calculated by Grundmann in and around a pyramidal InAs QD (Grundmann et al., 1995), there exist lateral potentials for electrons and holes in the vicinity of a QD. The potential for holes increases close to the QD and gives rise to a barrier for the capture of holes from the wetting layer (WL) in QD. On the other hand, the potential for electrons drops monotonically due to the weak influence. Therefore, the excited carriers in the WLs and the spacer layers lead to the transfer of an impaired hole into the QDs (Adler et al., 1996). In the lower temperature region, lateral coupling-like behaviour arises from the hole injection from the spacer layers. In our QD systems, there are two possible reasons causing the lateral coupling at lower temperature region: the high QD density and the decrease in the potential height due to strain compensation. The high QD density enables to transfer in-plane direction in

comparison with the vertical direction, and the strain compensation reduces the potential height induced by the lattice-mismatch strain. These two factors will lead the lateral coupling in the lower temperature comparably.

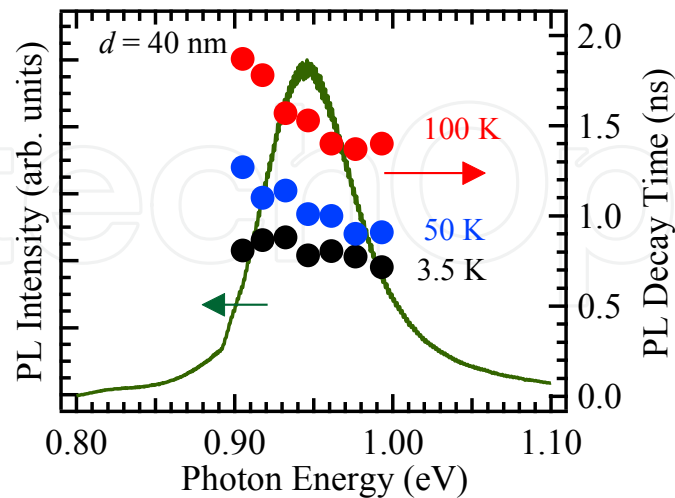


Fig. 7. Temperature dependence of the PL decay time and PL spectrum at 3.5 K in the $d=40$ nm sample.

To reveal the effects of the lateral coupling on the intraband transition process, we measured the excitation-energy dependence of the PL spectrum systematically. In measurements of the excitation-energy dependence, the excitation light was produced by combination of a 100-W Xe lamp and a 32-cm single monochromator with a resolution of 5 nm. The emitted light was dispersed by a 32-cm single monochromator with a resolution of 1.0 nm. In Fig. 8, the excitation-energy dependence of the PL intensity monitored at the PL peak energy

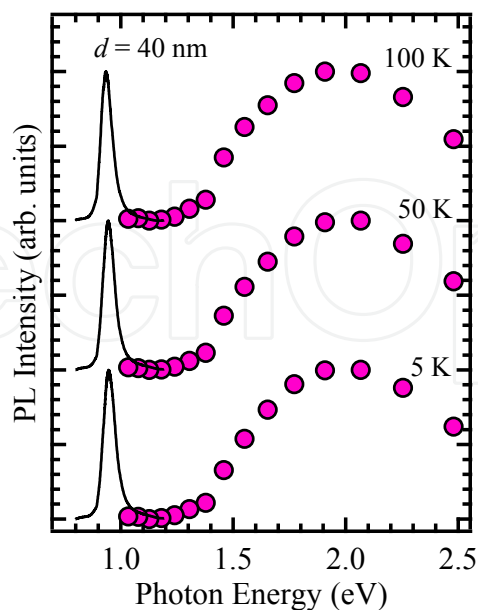


Fig. 8. Excitation-energy dependence of the PL peak intensity measured at various temperatures (circles) in the $d = 40$ nm sample. The PL spectrum at each temperature is also shown.

measured at various temperatures is depicted. All the profiles were normalized by the maximum intensity. All profiles show the maximum intensity around 1.9 eV. The bandgap energy of the InP substrate is 1.424 eV at 1.6 K and the $\text{In}_{0.5}\text{Ga}_{0.1}\text{Al}_{0.4}\text{As}$ spacer layer is around 1.357 eV at room temperature (Madelung, 2004). Therefore, the maximum intensity around 1.9 eV is attributed not to the resonant carrier injection from the spacer layers and substrates but to the higher-order excitons in InAs QDs. This demonstrates the existence of the above barrier exciton states around these energy regions. The profile of the excitation-energy dependence of the PL peak intensity hardly changes with the temperature. This result indicates that the lateral coupling is negligible for the intraband relaxation process in this sample.

Next, we discuss the relation between the interconnection effects along the growth direction and the lateral coupling. We performed the same experiments in the $d=20$ nm sample which has a longer exciton lifetime due to the interconnection effect as shown in Fig. 9. The increase factor of the PL decay time depending on the temperature is much larger than that in the $d=40$ nm sample. This result indicates that the lateral coupling effect affects the carrier relaxation process in the $d=20$ nm sample. Therefore, intraband relaxation process will change with temperature.

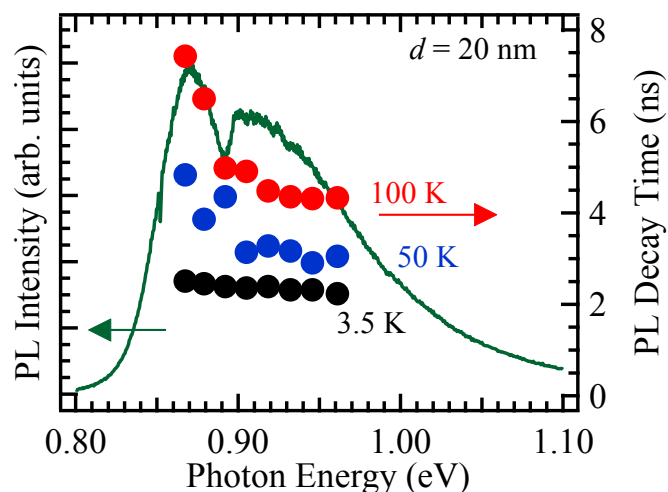


Fig. 9. Temperature dependence of the PL decay time and PL spectrum at 3.5 K in the $d=20$ nm sample.

Figure 10 shows the excitation-energy dependence of the PL peak intensity measured at various temperatures in the $d=20$ nm sample (Kojima et al., 2011). The PL spectrum at each temperature is also shown. The profiles show the peak around 1.5 eV. The difference of the peak energy between the $d=40$ nm and $d=20$ nm samples comes from that of the lowest exciton energy. While the dependence of the PL intensity in the $d=40$ nm sample hardly changes, that in the $d=20$ nm sample clearly changes around the higher energy over 1.6 eV. This change is related to the exciton lifetime. As mentioned above, the exciton lifetime in the $d=40$ nm ($d=20$ nm) sample is 0.8 (1.9) ns. When the exciton lifetime is shorter than the transfer time under the lateral coupling conditions, the transfer process does not have a sufficient effect on the intraband relaxation process. On the other hand, in the case that the exciton lifetime is longer than the transfer time, the transfer process changes the intraband relaxation process, because it will be difficult for the transferred carriers to relax into the

QDs because of the occupied states. Therefore, the carriers generated in the smaller QDs with the larger transition energies strongly affects the larger QDs with the smaller transition energies. However, for application of the QDs with longer exciton lifetime to optical devices, especially photo receiving devices such as the photodetectors or solar cells, the exciton transfer time is considered to be not as fast as the deteriorating carrier extraction.

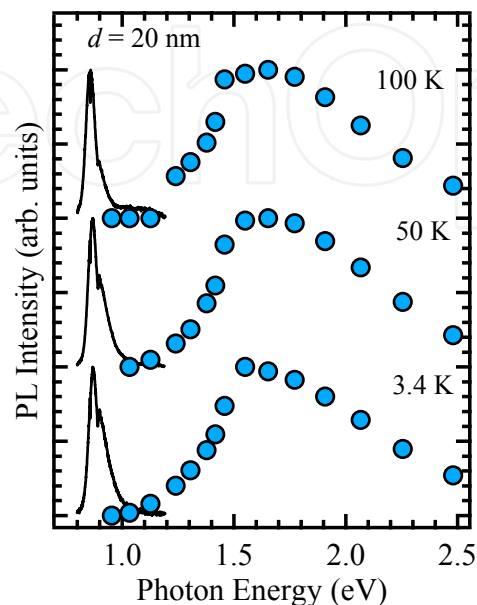


Fig. 10. Excitation-energy dependence of the PL peak intensity measured at various temperatures (circles) in the $d = 20$ nm sample. The PL spectrum at each temperature is also shown.

5. Conclusion

We have investigated the PL characteristics of excitons in multilayer stacked QDs with different spacer layer thicknesses. We found that the intensity of the PL band decreases with a decrease in spacer layer thickness. The PL spectra in the thinner spacer layer sample indicate the elongation of electron envelope functions along the growth direction. Moreover, from the PL decay time, it is revealed that the elongation of the electron envelope functions induces the lowering of an oscillator strength, leading to the lengthening of the PL decay time. This result suggests the interconnection of QDs along the growth direction via the overlap of the electron envelope functions. It is concluded that the PL characteristics of stacked QDs can be controlled by altering the spacer layer thickness through the variation of the exciton oscillator strength.

In addition, we have investigated the effects of temperature on the PL characteristics of excitons in the $d=40$ nm and $d=20$ nm samples. We found that the decrease in the PL intensity in the $d=20$ nm sample with interconnection effect is similar to that in the $d=40$ nm sample. To clarify the effect of the interconnection in the $d=20$ nm sample, we examined the temperature dependence of the PL decay time. The PL decay profiles, which show the increase in the PL decay time with temperature, indicated the suppression of nonradiative recombination paths caused during the QD and spacer layer growth processes. The increase in the PL decay time arises from the thermal delocalization.

However, the temperature dependence of the PL decay time in the two samples is different. In order to reveal the discrepancy in the temperature dependence of the PL characteristics, we examined the detection energy dependence of the PL decay time. The PL decay times of both samples clearly depend on the detection energy; this indicates the lateral coupling between the QDs. As the temperature increases, the excitons transfer from smaller QDs to larger ones. This affects the exciton relaxation process. However, in the $d=20$ nm sample, the vertical interaction in addition to the lateral interaction strongly affects the excitonic process, and therefore, the temperature dependence of the PL decay time differs from that in the $d=40$ nm sample.

Finally, we investigated the effect of the lateral coupling, namely the exciton/carrier transfer process in the in-plane direction, on the intraband relaxation process of photoexcited carriers in $d=20$ nm and $d=40$ nm samples. The detection-energy dependence of the PL decay time indicates the in-plane interaction between QDs even at 50 K in both the samples. In the excitation-energy dependence of the PL intensity, while the transfer process hardly changes the intraband relaxation process in the $d=40$ nm sample, that in the $d=20$ nm sample changes the intraband relaxation process. Because the exciton lifetime in the $d=20$ nm sample is longer than that in the $d=40$ nm sample, this change depends on the exciton lifetime.

These findings suggest that the interconnection of QDs along the growth direction via the overlapping of electron envelope functions occurs at high temperatures. These may aid the development of some functional devices by using QDs. In particular, they will be advantageous for the devices based on the so-called QD superlattice.

6. Acknowledgment

We would like to thank Dr. K. Akahane from National Institute of Information and Communications Technology, Japan, Prof. O. Wada, Prof. T. Kita, Mr. H. Nakatani, and Mr. M. Mamizuka from Kobe University for their fruitful discussions. These works were partially supported by the Grant-in-Aid for the Scientific Research and from the Ministry of Education, Culture, Sports, Science, and Technology of Japan (No.23656050).

7. References

- Adler, F.; Geiger, M.; Bauknecht, A.; Scholz, F.; Schweizer, H.; Pilkuhn, M. H.; Ohnesorge, B. & Forchel, A. (1996) Optical transitions and carrier relaxation in self assembled InAs/GaAs quantum dots. *Journal of Applied Physics* Vol. 80, No. 7, pp. 4019-4026, ISSN 0021-8979
- Akahane, K.; Ohtani, N.; Okada, Y. & Kawabe, M. (2002) Fabrication of ultra-high density InAs-stacked quantum dots by strain-controlled growth on InP(311)B substrate. *Journal of Crystal Growth* Vol. 245, No. 1-2, pp. 31-36, ISSN 0022-0248
- Akahane, K.; Yamamoto, N. & Tsuchiya, M. (2008) Highly stacked quantum-dot laser fabricated using a strain compensation technique. *Applied Physics Letters* Vol. 93, No. 4, pp. 041121-1-3, ISSN 0003-6951
- Akahane, K.; Yamamoto, N. & Kawanishi, T. (2011) Fabrication of ultra-high-density InAs quantum dots using the strain-compensation technique. *Physica Status Solidi A* Vol. 208, No. 2, pp. 425-428, ISSN 1862-6300

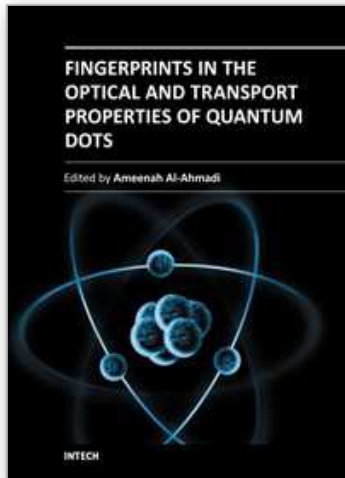
- Akiyama, H.; Koshihara, S.; Someya, T.; Wada, K.; Noge, H.; Nakamura, Y.; Inoshita, T.; Shimizu, A. & Sakaki, H. (1994) Thermalization effect on radiative decay of excitons in quantum wires. *Physical Review Letters* Vol. 72, No. 6, pp. 924-927, ISSN 1079-7114
- Andreani, L. C.; Panzarini, G. & Gerard, J.-M. (1999) Strong-coupling regime for quantum boxes in pillar microcavities: Theory. *Physical Review B* Vol. 60, No. 19, pp. 13276-13279, ISSN 1098-0121
- Arakawa, Y. & Sakaki, H. (1982) Multidimensional quantum well laser and temperature dependence of its threshold current. *Applied Physics Letters* Vol. 40, No. 11, pp. 939-941, ISSN 0003-6951
- Bardot, C.; Schwab, M.; Bayer, M.; Farad, S.; Wasilewski, Z. & Hawrylak, P. (2005) Exciton lifetime in InAs/GaAs quantum dot molecules. *Physical Review B* Vol. 72, No. 3, pp. 035314-1-7, ISSN 1098-0121
- Bogaart, E. W.; Nötzel, R.; Gong, Q.; Haverkort, J. E. M. & Wolter, J. H. (2005) Ultrafast carrier capture at room temperature in InAs/InP quantum dots emitting in the 1.55 μm wavelength region. *Applied Physics Letters* Vol. 86, No. 17, pp.173109-1-3, ISSN 0003-6951
- Brandt, O.; Tapfer, L.; Ploog, K.; Bierwolf, R. & Hohenstein, M. (1992) Effect of In segregation on the structural and optical properties of ultrathin InAs films in GaAs. *Applied Physics Letters* Vol. 61, No. 23, pp.2814-2816, ISSN 0003-6951
- Fiore, A.; Borri, P.; Langbein, W.; Hvam, J. M.; Oesterie, U.; Houdré, R.; Stanley, R. P. & Illegems, M. (2000) Time-resolved optical characterization of InAs/InGaAs quantum dots emitting at 1.3 μm . *Applied Physics Letters* Vol. 76, No. 23, pp.3430-3432, ISSN 0003-6951
- Goldstein, L.; Glas, F.; Marzin, J. Y.; Charasse, M. N. & Le Roux, G. (1985) Growth by molecular beam epitaxy and characterization of InAs/GaAs strained-layer superlattices. *Applied Physics Letters* Vol. 47, No. 10, pp.1099-1101, ISSN 0003-6951
- Grundmann, M.; Stier, O. & Bimberg, D. (1995) InAs/GaAs pyramidal quantum dots: Strain distribution, optical phonons, and electronic structure. *Physical Review B* Vol. 52, No. 16, pp. 11969-11981, ISSN 1098-0121
- Hostein, R.; Michon, A.; Beaudoin, G.; Gogneau, N.; Patriache, G.; Marzin, J.-Y.; Robert-Phillip, I.; Sagnes, I. and Beveratos, A. (2008) *Applied Physics Letters* Vol. 93, No. 7, pp.073106-1-3, ISSN 0003-6951
- Hours, J.; Senellart, P.; Peter, E.; Cavanna, A. & Bloch, J. (2005) Exciton radiative lifetime controlled by the lateral confinement energy in a single quantum dot. *Physical Review B* Vol. 71, No. 16, pp. 161306-1-4, ISSN 1098-0121
- Huffaker, D. L.; Park, G.; Zou, Z.; Shchekin, O. B. & Deppe D. G. (1998) 1.3 μm room-temperature GaAs-based quantum-dot laser. *Applied Physics Letters* Vol. 73, No. 18, pp. 2564-2566, ISSN 0003-6951
- Inoue, T.; Kita, T.; Wada, O.; Konno, M.; Yaguchi, T. & Kamino, T. (2008) Electron tomography of embedded semiconductor quantum dot. *Applied Physics Letters* Vol. 92, No. 3, pp. 031902-1-3, ISSN 0003-6951
- Kayanuma, Y. (1988) Quantum-size effects of interacting electrons and holes in semiconductor microcrystals with spherical shape. *Physical Review B* Vol. 38, No. 14, pp. 9797-9805, ISSN 1098-0121

- Kim, J. S.; Lee, J. H.; Hong, S. U.; Han, W. S.; Kwack, H.-S. & Oh, D. K. (2003) Influence of InGaAs overgrowth layer on structural and optical properties of InAs quantum dots. *Journal of Crystal Growth* Vol. 255, No. 1-2, pp. 57-62, ISSN 0022-0248
- Kojima, O.; Nakatani, H.; Kita, T.; Wada, O.; Akahane, K. & Tsuchiya, M. (2008) Photoluminescence characteristics of quantum dots with electronic states interconnected along growth direction. *Journal of Applied Physics* Vol. 103, No. 11, pp. 113504-1-5, ISSN 0021-8979
- Kojima, O.; Nakatani, H.; Kita, T.; Wada, O. & Akahane, K. (2010) Temperature dependence of photoluminescence characteristics of excitons in stacked quantum dots and quantum dot chains. *Journal of Applied Physics* Vol. 107, No. 11, pp. 073506-1-4, ISSN 0021-8979
- Kojima, O.; Mamizuka, M.; Kita, T.; Wada, O. & Akahane, K. (2011) Intraband relaxation process in highly stacked quantum dots. *Physica Status Solidi C* Vol. 8, No. 1, pp. 46-49, ISSN 1610-1642
- Madelung, O. (2004) *Semiconductors: Data Handbook*, Springer-Verlag, ISBN 978-3540404880
- Martí, A.; Antolín, E.; Stanley, C. R.; Farmer, C. D.; López, N.; Díaz, P.; Cánovas, E.; Linares, P. G. & Luque, A. (2006) Production of photocurrent due to intermediate-to-conduction-band transitions: a demonstration of a key operating principle of the intermediate-band solar cell. *Physical Review Letters* Vol. 97, No. 24, pp. 247701-1-4, ISSN 1079-7114
- Nakatani, H.; Kita, T.; Kojima, O.; Wada, O.; Akahane, K. & Tsuchiya, M. (2008) Photoluminescence dynamics of coupled quantum dots. *Journal of Luminescence* Vol. 128, No. 5-6, pp. 975-977, ISSN 0022-2313
- Oshima, R.; Takata, A. & Okada, Y. (2008) Strain-compensated InAs/GaNAs quantum dots for use in high-efficiency solar cells. *Applied Physics Letters* Vol. 93, No. 8, pp. 083111-1-3, ISSN 0003-6951
- Persson, J.; Håkanson, U.; Johansson, M. K.-J.; Samuelson, L. & Pistol, M.-E. (2005) Strain effects on individual quantum dots: Dependence of cap layer thickness. *Physical Review B* Vol. 72, No. 8, pp. 085302-1-2, ISSN 1098-0121
- Prasanth, R.; Haverkort, J. E. M.; Deepthy, A.; Bogaart, E. W.; van der Tol, J. J. G. M.; Patent, E. A.; Zhao, G.; Gong, Q.; van Veldhoven, P. J.; Nötzel, R. & Wolter, J. H. (2004) All-optical switching due to state filling in quantum dots. *Applied Physics Letters* Vol. 84, No. 20, pp. 4059-4061, ISSN 0003-6951
- Saito, H.; Nishi, K. & Sugou, S. (1998) Influence of GaAs capping on the optical properties of InGaAs/GaAs surface quantum dots with 1.5 μm emission. *Applied Physics Letters* Vol. 73, No. 19, pp. 2742-2744, ISSN 0003-6951
- Saito, T.; Nakaoka, T.; Kakitsuka, T.; Yoshikuni, Y. & Arakawa, Y. (2005) Strain distribution and electronic states in stacked InAs/GaAs quantum dots with dot spacing 0–6 nm. *Physica E: Low-dimensional Systems and Nanostructures* Vol. 26, No. 1-4, pp. 217-221, ISSN 1386-9477
- Takagahara, T. (1987) Excitonic optical nonlinearity and exciton dynamics in semiconductor quantum dots. *Physical Review B* Vol. 36, No. 17, pp. 9293-9296, ISSN 1098-0121
- Wang, G.; Fafard, S.; Leonard, D.; Bowers, J. E.; Merz, J. L. & Petroff, P. M. (1994) Time-resolved optical characterization of InGaAs/GaAs quantum dots. *Applied Physics Letters* Vol. 64, No. 21, pp. 2815-2817, ISSN 0003-6951

- Xie, Q.; Chen, P.; Kalburge, A.; Ramachandran, T. R.; Nayfonov, A.; Konkar, A. & Madhukar, A. (1995) Realization of optically active strained InAs island quantum boxes on GaAs(100) via molecular beam epitaxy and the role of island induced strain fields. *Journal of Crystal Growth* Vol. 150, No. 1, pp. 357-363, ISSN 0022-0248
- Yu, H.; Lycett, S.; Roberts, C. & Murray, R. (1996) Time resolved study of self-assembled InAs quantum dots. *Applied Physics Letters* Vol. 69, No. 26, pp. 4087-4089, ISSN 0003-6951

IntechOpen

IntechOpen



Fingerprints in the Optical and Transport Properties of Quantum Dots

Edited by Dr. Ameenah Al-Ahmadi

ISBN 978-953-51-0648-7

Hard cover, 468 pages

Publisher InTech

Published online 13, June, 2012

Published in print edition June, 2012

The book "Fingerprints in the optical and transport properties of quantum dots" provides novel and efficient methods for the calculation and investigating of the optical and transport properties of quantum dot systems. This book is divided into two sections. In section 1 includes ten chapters where novel optical properties are discussed. In section 2 involve eight chapters that investigate and model the most important effects of transport and electronics properties of quantum dot systems This is a collaborative book sharing and providing fundamental research such as the one conducted in Physics, Chemistry, Material Science, with a base text that could serve as a reference in research by presenting up-to-date research work on the field of quantum dot systems.

How to reference

In order to correctly reference this scholarly work, feel free to copy and paste the following:

Osamu Kojima (2012). Exciton Dynamics in High Density Quantum Dot Ensembles, Fingerprints in the Optical and Transport Properties of Quantum Dots, Dr. Ameenah Al-Ahmadi (Ed.), ISBN: 978-953-51-0648-7, InTech, Available from: <http://www.intechopen.com/books/fingerprints-in-the-optical-and-transport-properties-of-quantum-dots/optical-characteristics-of-high-density-quantum-dot>

INTECH
open science | open minds

InTech Europe

University Campus STeP Ri
Slavka Krautzeka 83/A
51000 Rijeka, Croatia
Phone: +385 (51) 770 447
Fax: +385 (51) 686 166
www.intechopen.com

InTech China

Unit 405, Office Block, Hotel Equatorial Shanghai
No.65, Yan An Road (West), Shanghai, 200040, China
中国上海市延安西路65号上海国际贵都大饭店办公楼405单元
Phone: +86-21-62489820
Fax: +86-21-62489821

© 2012 The Author(s). Licensee IntechOpen. This is an open access article distributed under the terms of the [Creative Commons Attribution 3.0 License](#), which permits unrestricted use, distribution, and reproduction in any medium, provided the original work is properly cited.

IntechOpen

IntechOpen